

Moment Propagation Through Carleman Linearization with Application to Probabilistic Safety Analysis

Sasinee Pruekprasert^a, Jeremy Dubut^{a,b}, Toru Takisaka^a, Clovis Eberhart^{a,b},
Ahmet Cetinkaya^a

^aNational Institute of Informatics, Tokyo, 101-8430, Japan

^bJapanese-French Laboratory of Informatics, IRL 3527, CNRS, Tokyo, Japan

Abstract

We develop a method to approximate the moments of a discrete-time stochastic polynomial system. Our method is built upon Carleman linearization with truncation. Specifically, we take a stochastic polynomial system with finitely many states and transform it into an infinite-dimensional system with linear deterministic dynamics, which describe the exact evolution of the moments of the original polynomial system. We then truncate this deterministic system to obtain a finite-dimensional linear system, and use it for moment approximation by iteratively propagating the moments along the finite-dimensional linear dynamics across time. We provide efficient online computation methods for this propagation scheme with several error bounds for the approximation. Our result also shows that precise values of certain moments can be obtained when the truncated system is sufficiently large. Furthermore, we investigate techniques to reduce the offline computation load using reduced Kronecker power. Based on the obtained approximate moments and their errors, we also provide probability bounds for the state to be outside of given hyperellipsoidal regions. Those bounds allow us to conduct probabilistic safety analysis online through convex optimization. We demonstrate our results on a logistic map with stochastic dynamics and a vehicle dynamics subject to stochastic disturbance.

Key words: Stochastic systems, nonlinear systems, probabilistic safety analysis, moment computation, Carleman linearization

1 Introduction

Uncertainty is one of the critical issues that make safety assurance of cyber-physical systems a difficult task. Handling uncertainty in automated driving systems is especially challenging, as motion planning algorithms are required to take account of uncertainty in both the measurement and the actuation mechanisms (Bry and Roy, 2011). Depending on the dynamical variations in the environment and the vehicle-controller interaction, the actual trajectory taken by a vehicle may differ substantially from a trajectory that is precomputed based on nominal dynamics of the vehicle. Most mo-

tion planning algorithms address this issue by assessing the collision risk for a set of possible future trajectories of the vehicle and not just for the nominal trajectory. Moreover, there are different approaches regarding how the uncertainty is modeled. A well known approach is based on considering known deterministic bounds on the disturbance and the measurement noise (see Althoff and Dolan (2014), and the references therein). Another approach is to use stochastic system models to describe the effects of uncertainty.

The effect of uncertainty on the state of a stochastic system can be quantified through the so-called *mean and covariance propagation* method. This method is especially effective for systems with linear dynamics where the uncertainty is modeled as additive Gaussian noise. For those systems, if the initial state distribution is Gaussian, the distribution of the state at any future time remains Gaussian. Moreover, the mean and the covariance of the state can be computed iteratively by using linear equations. Previously, Bry and Roy (2011) and Banzhaf *et al.* (2018) used this propagation method together with Kalman filters in motion planning tasks.

While mean and covariance propagation is an effective

* The authors are supported by ERATO HASUO Metamathematics for Systems Design Project No. JPMJER1603, JST; S. Pruekprasert is also supported by Grant-in-aid No. 21K14191, JSPS. J. Dubut is also supported by Grant-in-aid No. 19K20215, JSPS. A. Cetinkaya is also supported by Grant-in-aid No. 20K14771, JSPS. Part of the material in this paper was presented at the 21st IFAC World Congress, Berlin, Germany.

Email addresses: sasinee@nii.ac.jp (Sasinee Pruekprasert), dubut@nii.ac.jp (Jeremy Dubut), takisaka@nii.ac.jp (Toru Takisaka), eberhart@nii.ac.jp (Clovis Eberhart), cetinkaya@nii.ac.jp (Ahmet Cetinkaya).

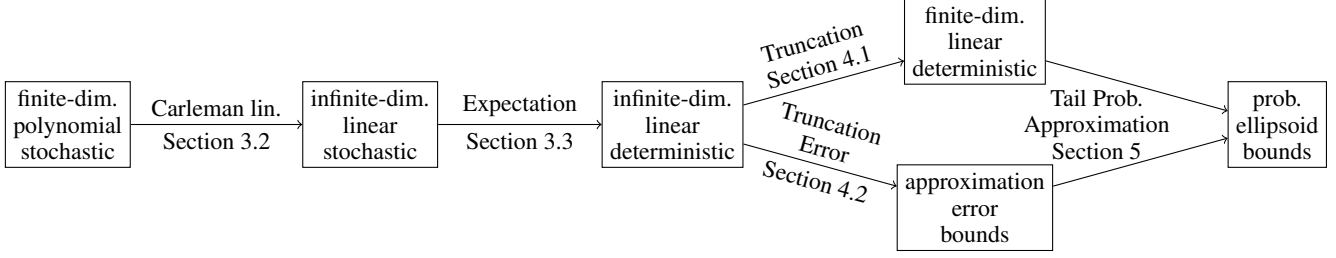


Fig. 1. The different steps of the proposed method

method for linear Gaussian systems, many cyber-physical systems involve nonlinearities and the noise cannot always be modeled as additive and Gaussian. Our goal in this paper is to develop a propagation method for nonlinear systems where the noise can be non-additive and non-Gaussian. Specifically, our propagation method can approximate the mean, covariance, and higher moments of such systems. We consider discrete-time stochastic nonlinear systems with polynomial dynamics, where the coefficients are randomly varying. Our model can describe both additive and multiplicative noise. Our propagation method is based on Carleman linearization with truncation (Steeb and Wilhelm, 1980). By following the Carleman linearization technique, we obtain a new dynamical system that describes how the Kronecker powers of the system state evolve. This system is linear, but it is infinite-dimensional. The expectation of the states of this linear system correspond to all moments of the original nonlinear system. By truncating the expected dynamics of the linear system at a certain truncation limit, we obtain a finite-dimensional linear system. Using the equations of this finite-dimensional system, our method iteratively computes the approximations of the moments of the nonlinear system up to the provided truncation limit.

The mean, the covariance, and higher moments of a system can provide useful statistical information regarding possible future state trajectories and can be used in safety verification. In this paper, we use our moment approximation method as a basis for developing a stochastic safety verification framework. Our framework uses tail probability bounds (Gray and Wang, 1991). In particular, we provide bounds on the probability for the state to be outside of a given hyperellipsoidal safety region, which we characterize using positive-semidefinite matrices. Previously, a scenario-based approach was used by Shen *et al.* (2020) to obtain similar safety regions for vehicles. This scenario-based approach is different from our moment-based approach: it relies on generating sufficiently many sample state trajectories using the information of the distributions of random elements in the dynamics. In our approach, we do not need to generate sample trajectories.

In this paper, we propose a novel tail probability-based safety verification framework consisting of two phases. The first one is an offline computation phase to compute the approximate moment dynamics and compute the upper bounds for their errors. The second phase is a fast online computation

to propagate the moments and their errors through the truncated dynamics, then use them to compute probabilistic ellipsoid bounds. A key ingredient in our framework is to efficiently compute bounds on moment approximation errors. First, we present the exact approximation error for a particular moment as a sum. However, for the exact computation, the number of terms is a quickly growing function of the dimension of the system and the time. We provide efficient on-line computation methods for this propagation scheme with several error bounds for the approximation. Furthermore, we investigate novel techniques to reduce the offline computation load using reduced Kronecker power, whose notion was also presented in (Bellman, 1970) and (Carravetta *et al.*, 1996) but used for different problems.

We present two case studies to demonstrate various aspects of our method. Our first case study is on a scalar stochastic logistic map. In particular, we consider uniformly distributed growth/decay rates in the dynamics. We run moment approximation and tail probability-based safety analysis. In the safety analysis, we check the conservativeness of our tail-probability bounds through Monte Carlo simulations. We observe that our obtained safety regions are quite tight for small durations. We also observe that our method is advantageous in terms of speed. It does not require drawing random variables, and as a result, it is much faster than Monte Carlo simulations even with small number of samples. Another advantage of our method is that it provides a theoretical guarantee for obtaining the safety regions.

Our second case study is on a vehicle with kinematic bicycle model. First, we use second-order Taylor expansion to obtain a discrete-time nonlinear polynomial system describing the vehicle. Then we use our approximate moment propagation approach to study how the vehicle's future states are affected by the uncertainty in the acceleration and in the initial vehicle state. Our approach uses the moments of the initial state of the vehicle and the moments for the acceleration to approximate future moments of the state. Here the uncertainty in the initial state is caused by the measurement noise and thus initial state moments are derived from the statistical properties of the measurement error. On the other hand uncertainty in the acceleration is related to actuators and the environment. In a typical control loop, our approach can be applied in a receding horizon fashion. In particular, computation is done by first obtaining new state measurements which are used for specifying the moments of the

new “initial” state; then these moments are propagated to approximately compute the moments of the state associated with future time instants.

The rest of the paper is organized as follows (see also Figure 1 for the specific sections where the main steps of the method are presented). Section 2 presents related work on Carleman linearization. In Section 3, we start from a finite-dimensional stochastic polynomial system, on which we apply the Carleman linearization technique to get an infinite-dimensional linear stochastic system. Then, we turn the linear stochastic system into a deterministic one by taking expectation. We present our truncation-based moment approximation method and study the error it introduces in Section 4, in which we also give an application of this bound. Then, in Section 5, we provide probabilistic ellipsoid bounds based on approximations of the first and second moments. Section 6 presents techniques to reduce the offline computation load using the concept of reduced Kronecker power. We provide two numerical examples to demonstrate the applicability of our approach in Section 7. Finally, in Section 8, we conclude the paper.

2 Related Work

The characterization of the dynamics under truncated Carleman linearization and the truncation error analysis in Section 3 appeared previously in our preliminary conference report (Pruekprasert *et al.*, 2020). Here in this paper, we present new results on tail-probability analysis in Section 5 and provide new techniques to improve the computational efficiency of our methods in Section 6. Moreover, we also provide a new upper bound for the approximation error from truncation in Section 4.3.3, using partial exact computation with indices on moment coordinates. We illustrate these new results and techniques in Section 7 through new simulations for a case study on vehicle dynamics.

The Carleman linearization technique is well-known in the nonlinear systems literature. For deterministic systems, it has been used for approximation of nonlinear models by linear ones (Bellman and Richardson, 1963; Steeb and Wilhelm, 1980; Al-Tuwaim *et al.*, 1998). Recently, Amini *et al.* (2019) used a Carleman linearization approach to design state feedback controllers for continuous-time nonlinear polynomial systems. Moreover, Hashemian and Armaou (2019) used Carleman linearization in model predictive control of continuous-time deterministic nonlinear systems. More recently, Amini *et al.* (2020) proposed an optimal control framework based on Carleman linearization. There, an approach using Carleman linearization with truncation allows the authors to approximately represent the Hamilton-Jacobi-Bellman equation (arising in optimal control of nonlinear systems) as an operator equation in quadratic form. This representation is then used to derive the approximate value function of the optimal control system as a quadratic Lyapunov function. The main advantage of the method is that it yields an iterative procedure to approximate the

value function that converges to the true value. In our work, we do not investigate the optimal control problem and we use Carleman linearization with truncation to approximate moments of stochastic systems instead of value functions.

There are fewer results on Carleman linearization for stochastic systems compared to deterministic ones. Specifically, Wong (1983) investigated bilinear noise terms in Ito-type stochastic differential equations and used Carleman linearization to describe how the moments of the stochastic differential equations evolve. Furthermore, Rauh *et al.* (2009) considered continuous-time nonlinear systems with additive noise and used a Carleman linearization technique in conjunction with a series expansion approach to approximate such systems with discrete-time linear systems. They then demonstrated that a Kalman filter can be used on the obtained linear systems for state estimation. In addition, Cacace *et al.* (2014) and Cacace *et al.* (2017) proposed Carleman linearization-based sampled-data filters for nonlinear stochastic differential equations driven by Wiener noise. More recently, Jasour *et al.* (2021) used a technique akin to Carleman linearization in moment propagation of a class of discrete-time mixed trigonometric polynomial systems with probabilistic disturbance. They show that several systems of interest are mixed trigonometric polynomial of degree 1, for which moment propagation without error is computationally feasible. The truncation error analysis in our paper is partly motivated by the work of Forets and Pouly (2017), which derives tight approximation error bounds for the truncated Carleman linearization of deterministic continuous-time systems. We note that deriving linear representations of finite-dimensional nonlinear systems can also be achieved through the use of Koopman operators (Goswami and Paley, 2017; Mesbahi *et al.*, 2019). A Koopman operator approach has recently been used in model predictive control of vehicles with deterministic nonlinear dynamics (Cibulka *et al.*, 2020).

Notations. We use \mathbb{N} for the set of non-negative integers. We denote by $M_1 \otimes M_2$ the Kronecker product of two matrices M_1 and M_2 . Moreover, we use $M^{[k]}$ to denote the k th Kronecker power of the matrix M , given by $M^{[0]} = 1$ and $M^{[k]} = M^{[k-1]} \otimes M$ for $k > 0$. The dimensions of the matrices we use grow rapidly, so we will use $n^{\leq k}$ as a shorthand for $\sum_{i=0}^k n^i$ when manipulating dimensions of vectors or matrices. We will sometimes write $\mathbb{E}[M]$ for a matrix $M = [m_{ij}]_{i \leq n, j \leq m}$ of random variables, by which we mean the matrix $[\mathbb{E}[m_{ij}]]_{i \leq n, j \leq m}$. For a matrix $M = [m_{ij}]_{i \leq n, j \leq m}$, we denote by $\|M\|_\infty$ its infinity norm, given by $\max_{i \leq n, j \leq m} |m_{ij}|$.

3 Carleman Linearization for Stochastic Polynomial Systems

In this section, we present the Carleman linearization technique to transform a finite-dimensional discrete-time stochastic polynomial system into an infinite-dimensional

one, then take expectation to get a deterministic system that describes the evolution of all moments of the system state.

3.1 Discrete-Time Stochastic Polynomial Systems

We consider the following finite-dimensional discrete-time stochastic polynomial system

$$\begin{aligned} x(t+1) &= \sum_{i=0}^{d_S} F_i(t) x^{[i]}(t), \quad t \in \mathbb{N}, \\ x(0) &= x_{\text{ini}}, \end{aligned} \quad (1)$$

where $x(t) \in \mathbb{R}^n$ is the state vector and $F_i(t) \in \mathbb{R}^{n \times n^i}$, $i \in \{0, 1, \dots, d_S\}$, are random matrices. More precisely, we assume given a probability space Ω , then the initial state vector x_{ini} (*resp.* vectors $x(t)$, $F_i(t)$) is a measurable function from Ω to \mathbb{R}^n (*resp.* \mathbb{R}^n , $\mathbb{R}^{n \times n^i}$). We consider the scenarios where all $F_i(t)$'s have known distributions.

Systems of the form (1) can be used to model dynamics with both additive and multiplicative noise terms. The vector $F_0(t) \in \mathbb{R}^n$ represents additive noise, as $x^{[0]}(t) = 1$, while the matrices $F_1(t), \dots, F_{d_S}(t)$ characterize the effects of multiplicative noise.

Let $F(t) \triangleq \begin{bmatrix} F_0(t) & F_1(t) & F_2(t) & \dots & F_{d_S}(t) \end{bmatrix} \in \mathbb{R}^{n \times n^{\leq d_S}}$. We make the following assumptions concerning the coefficient matrices and the random initial state x_{ini} .

Assumption 3.1. *The vector x_{ini} and the matrices $F(t)$, $t \in \mathbb{N}$, are all independent.*

Assumption 3.2. *The matrices $\{F(t) | t \in \mathbb{N}\}$ are identically distributed.*

Note that Assumptions 3.1 and 3.2 are not overly restrictive and they hold in fairly general situations as we discuss in Section 7. Notice also that under Assumption 3.1, matrices $F_i(t)$ and $F_j(t)$ are still allowed to statistically depend on each other. Moreover, Assumption 3.2 allows us to obtain a “time-invariant” method to compute moments, further yielding computational advantage.

Example 1. Consider

$$\begin{aligned} x_1(t+1) &= a(t)x_1(t)x_2(t), & x_1(0) &= x_{\text{ini},1}, \\ x_2(t+1) &= a(t)(x_1(t) + x_2(t)), & x_2(0) &= x_{\text{ini},2}, \end{aligned}$$

where $x_{\text{ini},1}$, $x_{\text{ini},2}$, and $a(t)$, $t \in \mathbb{N}$, are independent and identically distributed uniformly random variables. By using

$$x(t) = \begin{bmatrix} x_1(t) & x_2(t) \end{bmatrix}^\top, F_1(t) = \begin{bmatrix} 0 & 0 \\ a(t) & a(t) \end{bmatrix}, \text{ and } F_2(t) =$$

$\begin{bmatrix} 0 & a(t) & 0 & 0 \\ 0 & 0 & 0 & 0 \end{bmatrix}$, we can rewrite the system as in the form of (1), i.e.,

$$x(t) = F_1 x^{[1]}(t) + F_2 x^{[2]}(t). \quad (2)$$

Our objective is to approximate the moments of the state of system (1), which we will use in Section 5 to compute probabilistic safety areas for the state vector $x(t)$ at a given time t . For Example 1, given j and t , our objective is to approximate the moment $\mathbb{E}[x^{[j]}(t)]$. Note that the initial moments (e.g., $\mathbb{E}[x^{[j]}(0)]$) can be computed from the probability distribution of x_{ini} .

3.2 Carleman Linearization

We use Carleman linearization to obtain an infinite-dimensional linear system that describes the evolution of the Kronecker powers of the state vector $x(t)$. By defining

$$y(k, t) \triangleq \begin{bmatrix} 1 & x(t)^\top & x^{[2]}(t)^\top & \dots & x^{[k]}(t)^\top \end{bmatrix}^\top \in \mathbb{R}^{n^{\leq k}}, \quad (3)$$

the dynamical system (1) can be rewritten as

$$x(t+1) = F(t)y(d_S, t).$$

Therefore, for all $j \in \mathbb{N}$, we have

$$x^{[j]}(t+1) = (F(t)y(d_S, t))^{[j]}.$$

By using the *mixed-product property* of the Kronecker product (i.e., $(A \otimes B)(C \otimes D) = AC \otimes BD$; see Section 13.2 of Laub (2004)), we obtain

$$\begin{aligned} x^{[j]}(t+1) &= F^{[j]}(t)y^{[j]}(d_S, t) \\ &= \sum_{k=0}^{jd_S} \left(\sum_{(i_l)_{l \leq j} \in H_{j,k}} F_{i_1}(t) \otimes \dots \otimes F_{i_j}(t) \right) x^{[k]}(t), \end{aligned}$$

for $j \in \mathbb{N}$, where

$$H_{j,k} \triangleq \left\{ (i_l)_{l \leq j} \mid \sum_{l=1}^j i_l = k \text{ and } i_l \leq d_S \right\}.$$

We thus get the infinite-dimensional linear system

$$\begin{aligned} x^{[j]}(t+1) &= \sum_{k=0}^{jd_S} \left(\sum_{(i_l)_{l \leq j} \in H_{j,k}} \bigotimes_{m=1}^j F_{i_m}(t) \right) x^{[k]}(t), \\ x^{[j]}(0) &= x_{\text{ini}}^{[j]}, \end{aligned}$$

which describes the evolution of all Kronecker powers $x^{[0]}(t), x^{[1]}(t), \dots$ of the state $x(t)$.

In order to give a simpler description of the system, we introduce the matrices $A_{j,k}(t) \in \mathbb{R}^{n^j \times n^k}$ given by

$$A_{j,k}(t) \triangleq \sum_{(i_l)_{l \leq j} \in H_{j,k}} F_{i_1}(t) \otimes \dots \otimes F_{i_j}(t).$$

Note in particular that $A_{0,0}(t) = 1$ since there is only the empty sequence in $H_{0,0}$, and $A_{j,k}(t) = 0$ if $j = 0$ and $k > 0$ or $k > jd_S$ since $H_{j,k}$ is then empty. We also introduce, for all $N, M \in \mathbb{N}$, the matrix $A(t; N, M)$ defined by blocks as:

$$A(t; N, M) \triangleq \begin{bmatrix} A_{0,0}(t) & \dots & A_{0,M}(t) \\ \vdots & \ddots & \vdots \\ A_{N,0}(t) & \dots & A_{N,M}(t) \end{bmatrix} \in \mathbb{R}^{n^{\leq N} \times n^{\leq M}}.$$

Then, for any $k \in \mathbb{N}$, we have

$$\begin{aligned} y(k, t+1) &= \begin{bmatrix} 1 & x^{[1]}(t+1)^\top & \dots & x^{[k]}(t+1)^\top \end{bmatrix}^\top \\ &= A(t; k, kd_S) \begin{bmatrix} 1 & x^{[1]}(t)^\top & \dots & x^{[kd_S]}(t)^\top \end{bmatrix}^\top \\ &= A(t; k, kd_S) y(kd_S, t). \end{aligned} \quad (4)$$

Example 2. For the system (2) in Example 1,

$$x^{[2]}(t+1) = (F_1(t)x^{[1]}(t) + F_2(t)x^{[2]}(t))^{[2]}.$$

Thus, by Equation (4), we have

$$\begin{aligned} y(2, t+1) &= \begin{bmatrix} 1 & x^{[1]}(t+1)^\top & x^{[2]}(t+1)^\top \end{bmatrix}^\top \\ &= \begin{bmatrix} 1 & 0 & 0 & 0 & 0 \\ 0 & F_1 & F_2 & 0 & 0 \\ 0 & 0 & F_1 \otimes F_1 & F_1 \otimes F_2 & F_2^{[2]} \\ & & & + F_2 \otimes F_1 & \end{bmatrix} \begin{bmatrix} x^{[0]}(t) \\ x^{[1]}(t) \\ x^{[2]}(t) \\ x^{[3]}(t) \\ x^{[4]}(t) \end{bmatrix} \\ &= A(t; 2, 2 \cdot 2) y(2 \cdot 2, t). \end{aligned}$$

Recall that our objective is to approximate the moment $\mathbb{E}[x^{[j]}(t)]$ for given j and t . In the next section, we will consider a vector $\mathbb{E}[y(k, t)]$ which includes all moments $\mathbb{E}[x^{[j]}(t)]$ where $j \leq k$.

3.3 Moment Equations

We now derive the deterministic system that describes the evolution of the moments of $x(t)$ by taking expectation

in (4). This gives

$$\mathbb{E}[y(k, t+1)] = \mathbb{E}[A(t; k, kd_S) y(kd_S, t)].$$

By iteration of (4), we get that $y(kd_S, t)$ is given by

$$\begin{aligned} y(kd_S, t) &= A(t-1; kd_S, kd_S^2) \dots A(0; kd_S^t, kd_S^{t+1}) \\ &\quad \cdot y(kd_S^{t+1}, 0), \quad t \in \mathbb{N}. \end{aligned} \quad (5)$$

It follows from Assumption 3.1 that $A(t; k, kd_S)$ and $y(kd_S, t)$ in (4) are mutually independent. To see this, observe that $A(t; k, kd_S)$ is composed of the matrices $F_i(t)$, which are independent of x_{ini} and $F(t-1), \dots, F(0)$, which determine $y(kd_S, t)$ as given by (5).

It then follows that

$$\mathbb{E}[y(k, t+1)] = \mathbb{E}[A(t; k, kd_S)] \mathbb{E}[y(kd_S, t)].$$

Here again, to give a simpler description of the system, we introduce new matrices. Notice that the coefficients of the matrix $\mathbb{E}[A(t; N, M)]$ are products of the moments of coefficients of $F(t)$ and thus independent of t by Assumption 3.2. We denote this matrix by $E(N, M) \in \mathbb{R}^{n^{\leq N} \times n^{\leq M}}$, emphasizing the fact that it is independent of the time. Similarly, we denote by $E_{i,j} \in \mathbb{R}^{n^i \times n^j}$ the matrix $\mathbb{E}[A_{i,j}(t)]$. The equation above can thus be rewritten to give the following system

$$\begin{aligned} \mathbb{E}[x^{[j]}(t+1)] &= \sum_{k=0}^{jd_S} E_{j,k} \mathbb{E}[x^{[k]}(t)], \quad t \in \mathbb{N}, \\ \mathbb{E}[x^{[j]}(0)] &= \mathbb{E}[x_{\text{ini}}^{[j]}]. \end{aligned} \quad (6)$$

Since the matrices $E_{j,k}$ only depend on the moments of the matrices $F(\cdot)$, they can be computed offline.

4 Moment Approximation through Truncation

We will now introduce an approach that allows us to compute *approximations* of the moments of $x(t)$. This truncation approach is critical, as an exact computation of the moments is impossible from a practical point of view. Indeed, by (3), computing the first k moments at time t amounts to computing $\mathbb{E}[y(k, t)]$. So, by iteration of (6),

$$\mathbb{E}[y(k, t)] = E(k, kd_S) \dots E(kd_S^{t-1}, kd_S^t) \mathbb{E}[y(kd_S^t, 0)]. \quad (7)$$

As this indicates, exact computation of the first k moments requires the knowledge of matrices $E(k, kd_S), E(kd_S, kd_S^2), \dots, E(kd_S^{t-1}, kd_S^t)$ of exponentially increasing dimensions, making any practical computation unrealistic. We thus resort to a truncation approach where we fix a truncation limit and consider a matrix of fixed size to approximately compute the moments of $x(t)$.

4.1 Approximate Moments and the Truncated System

In this section, we define the system that we use to compute approximations of the moments of $x(t)$.

We fix $N_T \in \mathbb{N}$ and define $\tilde{x}_i(t) \in \mathbb{R}^{n_i}$, $i \in 1, \dots, N_T$, by

$$\begin{aligned} & \begin{bmatrix} 1 & \tilde{x}_1(t)^\top & \dots & \tilde{x}_{N_T}(t)^\top \end{bmatrix}^\top \\ &= E(N_T, N_T)^t \begin{bmatrix} 1 & \mathbb{E}[x_{\text{ini}}]^\top & \dots & \mathbb{E}[x_{\text{ini}}^{[N_T]}]^\top \end{bmatrix}^\top. \end{aligned} \quad (8)$$

Notice that (8) follows the same pattern as (7), but use the square matrix $E(N_T, N_T)$. Here, the vector $\tilde{x}_i(t)$ represents an approximation of the moment $\mathbb{E}[x^{[i]}(t)]$ that is computed using only our knowledge of the first N_T moments of x_{ini} .

By letting $\tilde{y}(t) \triangleq [1 \ \tilde{x}_1^\top(t) \ \tilde{x}_2^\top(t) \ \dots \ \tilde{x}_{N_T}^\top(t)]^\top$, we obtain what we call the “truncated system”, which is a discrete-time linear time-invariant system given by

$$\begin{aligned} \tilde{y}(t+1) &= E(N_T, N_T)\tilde{y}(t), \quad t \in \mathbb{N}, \\ \tilde{y}(0) &= [1 \ \mathbb{E}[x_{\text{ini}}(t)]^\top \ \dots \ \mathbb{E}[x_{\text{ini}}^{[N_T]}(t)]^\top]^\top. \end{aligned}$$

The truncated system allows us to iteratively compute approximations of the moments of $x(t)$ at consecutive time instants. Moreover, the approach only requires an offline computation of the matrix $E(N_T, N_T)$.

Example 3. By considering $N_T = 2$, we may approximate the first and the second moments of the system in Example 2 by the following truncated system.

$$\begin{aligned} \tilde{y}(t+1) &= [1 \ \tilde{x}_1^\top(t+1) \ \tilde{x}_2^\top(t+1)]^\top \\ &= \mathbb{E} \begin{bmatrix} 1 & 0 & 0 \\ 0 & F_1(t) & F_2(t) \\ 0 & 0 & F_1(t) \otimes F_1(t) \end{bmatrix} \begin{bmatrix} 1 \\ \tilde{x}_1^\top(t) \\ \tilde{x}_2^\top(t) \end{bmatrix} \\ &= E(2, 2)\tilde{y}(t), \end{aligned}$$

where $\tilde{x}_1^\top(0) = \mathbb{E}[x_{\text{ini}}(t)]^\top$ and $\tilde{x}_2^\top(0) = \mathbb{E}[x_{\text{ini}}^{[2]}(t)]^\top$.

4.2 Computation of Truncation Errors

We now consider the error due to the truncation. We consider $j_0 \in \{0, \dots, N_T\}$, and let $e_{j_0}(t) \in \mathbb{R}^{n^{j_0}}$ denote the error of the j_0 -th moment, that is,

$$e_{j_0}(t) \triangleq \mathbb{E}[x^{[j_0]}(t)] - \tilde{x}_{j_0}(t).$$

First, by (6), we have

$$\begin{aligned} \mathbb{E}[x^{[j_0]}(t)] &= \sum_{j_1=0}^{j_0 d_S} E_{j_0, j_1} \mathbb{E}[x^{[j_1]}(t-1)] \\ &= \sum_{j_1=0}^{j_0 d_S} E_{j_0, j_1} \sum_{j_2=0}^{j_1 d_S} E_{j_1, j_2} \mathbb{E}[x^{[j_2]}(t-2)] \\ &= \sum_{j_1=0}^{j_0 d_S} E_{j_0, j_1} \sum_{j_2=0}^{j_1 d_S} E_{j_1, j_2} \dots \sum_{j_t=0}^{j_{t-1} d_S} E_{j_{t-1}, j_t} \mathbb{E}[x_{\text{ini}}^{[j_t]}], \end{aligned}$$

and similarly, by (8),

$$\tilde{x}_{j_0}(t) = \sum_{j_1=0}^{N_T} E_{j_0, j_1} \sum_{j_2=0}^{N_T} E_{j_1, j_2} \dots \sum_{j_t=0}^{N_T} E_{j_{t-1}, j_t} \mathbb{E}[x_{\text{ini}}^{[j_t]}].$$

By observing that $E_{j,k} = 0$ for $k > j d_S$, we obtain from the two equations above,

$$\begin{aligned} e_{j_0}(t) &= \mathbb{E}[x^{[j_0]}(t)] - \tilde{x}_{j_0}(t) \\ &= \sum_{j_1=N_T+1}^{j_0 d_S} E_{j_0, j_1} \sum_{j_2=0}^{j_1 d_S} \dots \sum_{j_t=0}^{j_{t-1} d_S} E_{j_{t-1}, j_t} \mathbb{E}[x_{\text{ini}}^{[j_t]}] \\ &\quad + \sum_{j_1=0}^{N_T} E_{j_0, j_1} \sum_{j_2=N_T+1}^{j_1 d_S} \dots \sum_{j_t=0}^{j_{t-1} d_S} E_{j_{t-1}, j_t} \mathbb{E}[x_{\text{ini}}^{[j_t]}] \\ &\quad + \dots \\ &\quad + \sum_{j_1=0}^{N_T} E_{j_0, j_1} \dots \sum_{j_{t-1}=0}^{N_T} E_{j_{t-2}, j_{t-1}} \sum_{j_t=N_T+1}^{j_{t-1} d_S} E_{j_{t-1}, j_t} \mathbb{E}[x_{\text{ini}}^{[j_t]}]. \end{aligned} \quad (9)$$

As an immediate consequence, we get the following:

Proposition 4.1. Consider the truncated approximation of the moments of system (1) with truncation limit $N_T \in \mathbb{N}$. If $j_0 d_S^t \leq N_T$, then $\tilde{x}_{j_0}(t) = \mathbb{E}[x^{[j_0]}(t)]$.

Proof. We show that, if $j_0 d_S^t \leq N_T$, then $e_{j_0}(t) = 0$. To this end, it is enough to show that, for all lines of (9) and sequences (j_1, \dots, j_t) of relevant indices, at least one E_{j_{k-1}, j_k} is equal to 0. Let us pick the i th line and any sequence as above. In particular, $j_{i-1} d_S > N_T$, hence $j_{i-1} > j_0 d_S^{t-1} \geq j_0 d_S^{i-1}$, so there exists $k \in \{1, \dots, i-1\}$ such that $j_k > j_{k-1} d_S$, which proves the desired result. \square

This shows that, for large values of truncation limit N_T , the proposed method computes *exact* moments $\mathbb{E}[x^{[j_0]}(t)]$ for j_0 and t small enough. Note that this is due to the *discrete-time* nature of the finite-dimensional polynomial system (1).

In the continuous-time case, approximation errors cannot be avoided in general (Forets and Pouly, 2017).

Since $\mathbb{E}[x^{[j_0]}(t)] = \tilde{x}_{j_0}(t) + e_{j_0}(t)$, if $e_{j_0}(t)$ could efficiently be computed, then so would $\mathbb{E}[x^{[i]}(t)]$, and there would be no need in using the truncated system. However, the exact value of $e_{j_0}(t)$ is generally hard to compute. Therefore, in the following section, we provide upper bounds for $e_{j_0}(t)$.

4.3 Approximation of Error Bounds

We now investigate the approximation error introduced by truncation. For a given $j_0 \in \{0, \dots, N_T\}$, our goal is to obtain an upper bound to $\|e_{j_0}(t)\|_\infty$, which is the error on the j_0 -th moment introduced by the truncation.

Bounds of $\|e_i(t)\|_\infty$ allow us to use various techniques to study the distribution of the state at future time steps. We illustrate this in Section 5 by using tail probability approximations to compute a safety area, for which we know that the probability of the system landing outside that area is bounded by a predefined constant.

4.3.1 Global Error Bound

First, let $\xi \triangleq \max_{0 \leq j \leq j_0 d_S^t} \|\mathbb{E}[x_{\text{ini}}^{[j]}]\|_\infty$. Using ξ , we can derive bounds for $e_{j_0}(t)$ by first rewriting (9) as

$$e_{j_0}(t) = \sum_{j=0}^{j_0 d_S^t} \tilde{E}_j \mathbb{E}[x_{\text{ini}}^{[j]}], \quad (10)$$

where $\tilde{E}_j \in \mathbb{R}^{n^{j_0} \times n^j}$ is constructed by additions and multiplications of $E_{i,j}$, and thus can be computed offline (note that \tilde{E}_j is dependent on t , but we keep this implicit for readability). From this, we can derive a global bound

$$\|e_{j_0}(t)\|_\infty \leq \xi \sum_{j=0}^{j_0 d_S^t} \|\tilde{E}_j\|_\infty,$$

where $\sum_{j=0}^{j_0 d_S^t} \|\tilde{E}_j\|_\infty$ can be computed offline.

Observe that ξ can be efficiently computed in some cases. An obvious situation is when the position x_{ini} is determined, in which case we have $\xi = \max\{1, \|x_{\text{ini}}\|_\infty^{j_0 d_S^t}\}$. Another case is when x_{ini} obeys a well-known distribution whose moments are easy to compute, such as uniform or normal distributions. Nevertheless, another case is when the system satisfies $x(t) \in \mathbb{R}$ and $0 \leq x_{\text{ini}} \leq 1$, in which case $\|\mathbb{E}[x_{\text{ini}}^{[j]}]\|_\infty$ is decreasing and we have $\xi = \|\mathbb{E}[x_{\text{ini}}^{[0]}]\|_\infty = 1$.

4.3.2 Error Bound using Partial Exact Computation with Block Indices on Moments

We can further refine (10) to consider a single line $i \leq n^{j_0}$ of this equation, for which we get

$$(e_{j_0}(t))_i = \sum_{j=0}^{j_0 d_S^t} v_{j,i} \mathbb{E}[x_{\text{ini}}^{[j]}], \quad (11)$$

where $v_{j,i} \in \mathbb{R}^{1 \times n^j}$ is the i th row of \tilde{E}_j . By repeated application of triangle and Cauchy-Schwarz inequalities, we obtain

$$|(e_{j_0}(t))_i| \leq \xi \sum_{j=0}^{j_0 d_S^t} \|v_{j,i}\|_\infty, \quad (12)$$

where $\sum_{j=0}^{j_0 d_S^t} \|v_{j,i}\|_\infty$ can also be computed offline.

This bound can, however, be crude in practice as the norm gets distributed over all sums and products. We alleviate this problem in the following proposition where we compute tighter bounds while maintaining a reasonable computational cost.

Proposition 4.2. *For any subset $J \subseteq \{0, \dots, j_0 d_S^t\}$, we have the bound*

$$|(e_{j_0}(t))_i| \leq \left| \sum_{j \in J} v_{j,i} \mathbb{E}[x_{\text{ini}}^{[j]}] \right| + \xi_J \sum_{j \notin J} \|v_{j,i}\|_\infty,$$

where $\xi_J = \max_{j \notin J} \|\mathbb{E}[x_{\text{ini}}^{[j]}]\|_\infty$.

The idea is that J is a set of indices where one should avoid distributing the norm over the sum. One should pick J to consist of those indices where the distribution is too crude and makes the error bound loose. In order for this method to be computationally efficient, one should pick J that is of relatively small size, e.g., $|J| = \mathcal{O}(t)$. One possible way to choose J is to fix a size \hat{j} and return the set of \hat{j} indices j where $\|v_{j,i}\|$ is the largest; another way is to return the set of \hat{j} indices j such that $\|\mathbb{E}[x_{\text{ini}}^{[j]}]\|_\infty$ is the largest. For example, suppose x_{ini} is drawn from a truncated normal distribution over the interval $[0, 1]$. Then $\xi = 1$ and $\xi_J = \|\mathbb{E}[x_{\text{ini}}^{[j_{\min}]}]\|_\infty$, where j_{\min} is the smallest number that is not in J . In particular, if J is chosen as the set of \hat{j} indices such that $\|\mathbb{E}[x_{\text{ini}}^{[j_{\min}]}]\|$ is largest among $j = 0, \dots, j_0 d_S^t$, then we have $J = \{0, \dots, [\hat{j}] - 1\}$ and $\xi_J = \|\mathbb{E}[x_{\text{ini}}^{[[J]]}]\|_\infty$.

4.3.3 Error Bound using Partial Exact Computation with Regular Indices on Moment Coordinates

We can further refine (10) and (11) by considering each element of matrix \tilde{E}_j and vector $\mathbb{E}[x_{\text{ini}}^{[j]}]$. Let $\tilde{v} = [\tilde{E}_0 \ \tilde{E}_1 \ \dots \ \tilde{E}_{j_0 d_S^t}]$ and $\tilde{y} = \mathbb{E}[x_{\text{ini}}^{[0]\tau} \ x_{\text{ini}}^{[1]\tau} \ \dots \ x_{\text{ini}}^{[j_0 d_S^t]\tau}]^\top$. In the same way as in (12), we have

$$|(e_{j_0}(t))_i| \leq \sum_{k=0}^m |\tilde{v}_{i,k}| |\tilde{y}_k| \leq \max_{k \leq m} |\tilde{y}_k| \cdot \sum_{k=0}^m |\tilde{v}_{i,k}|,$$

where \tilde{y}_k is the k th row of \tilde{y} and $\tilde{v}_{i,k}$ is the element at i th row and k th column of \tilde{v} . Then, in the same way as in Proposition 4.2, we obtain the following proposition.

Proposition 4.3. *For any subset $K \subseteq \{0, \dots, m\}$, we have*

$$|(e_{j_0}(t))_i| \leq \left| \sum_{k \in K} \tilde{v}_{i,k} \tilde{y}_k \right| + \max_{k \notin K} |\tilde{y}_k| \sum_{k \notin K} |\tilde{v}_{i,k}|. \quad (13)$$

Again, one possible option of the set K is to fix a size \hat{k} and then choose \hat{k} indices k where $|\tilde{y}_k|$ is the largest.

In the next section, we will use these error bounds for probabilistic safety analysis.

5 Ellipsoid Bounds for Probabilistic Safety Analysis

Everything that we have computed up to this point can be computed offline, as it does not depend on the actual system state. In this section, we will show how to do online computation of probabilistic safety regions using tail probability analysis. It crucially relies on approximations of the first and second moments of the dynamics of the system.

5.1 Tail Probability Approximation

In this section, we use the bounds on the error introduced by the truncated system, which are derived in Section 4.3, to give a lower bound on the probability of the system being inside a given ellipsoid region after t time steps.

We define the region we are interested in terms of positive-semidefinite matrices. A matrix $P \in \mathbb{R}^{n \times n}$ is positive-semidefinite if, for all vectors $x \in \mathbb{R}^n$, $x^\top P x \geq 0$. Such a P defines a seminorm, called the P -seminorm, by $\|x\|_P = (x^\top P x)^{1/2}$. The region defined by $\|x\|_P \leq r$ is an ellipsoid (possibly of infinite radius in some dimensions).

Suppose we know some approximations $(\tilde{x}_2(t))_{ni+j}$ (henceforth denoted $(\tilde{x}_2(t))_{ij}$) of expectations $\mathbb{E}[x_i(t)x_j(t)]$ for all $i, j \leq n$ (where n is the dimension of the state space, as in (1)), with respective error bounds ε_{ij} , as well as

approximations $(\tilde{x}_1(t))_i$ of $\mathbb{E}[x_i(t)]$ with error bounds ε_i . Finally, assume that we know a global error bound $\|\tilde{x}_1(t) - \mathbb{E}[x(t)]\|_P \leq \varepsilon_P$. All these different bounds can be found by applying the techniques in Section 4.3, except for ε_P , which we discuss later.

We can then compute an upper-bound the probability to be outside of a “safe” ellipsoid region centered on $\tilde{x}_1(t)$ by the following proposition.

Proposition 5.1. *Let $\|\cdot\|_P$ be the P -seminorm. For $\alpha > \varepsilon_P$,*

$$\begin{aligned} \mathbb{P}(\|x(t) - \tilde{x}_1(t)\|_P \geq \alpha) \\ \leq \frac{\sum_{i,j=1}^n p_{ij} (\mathbb{E}[x_i(t)x_j(t)] - \mathbb{E}[x_i(t)]\mathbb{E}[x_j(t)])}{(\alpha - \varepsilon_P)^2}. \end{aligned} \quad (14)$$

Proof. Let $P = (p_{ij})_{i,j \leq n}$. Since $\alpha > \varepsilon_P$, we get by Markov’s inequality:

$$\begin{aligned} \mathbb{P}(\|x(t) - \tilde{x}_1(t)\|_P \geq \alpha) \\ \leq \mathbb{P}(\|x(t) - \mathbb{E}[x(t)]\|_P \geq \alpha - \varepsilon_P) \\ = \mathbb{P}(\|x(t) - \mathbb{E}[x(t)]\|_P^2 \geq (\alpha - \varepsilon_P)^2) \\ \leq \frac{\mathbb{E}[\|x(t) - \mathbb{E}[x(t)]\|_P^2]}{(\alpha - \varepsilon_P)^2} \\ = \frac{\sum_{i,j=1}^n p_{ij} (\mathbb{E}[x_i(t)x_j(t)] - \mathbb{E}[x_i(t)]\mathbb{E}[x_j(t)])}{(\alpha - \varepsilon_P)^2}. \quad \square \end{aligned}$$

Proposition 5.1 gives a means to bound the probability of the system being outside of an ellipsoid centered around $\tilde{x}_1(t)$.

For a fixed matrix P and known values of $\tilde{x}_1(t)_i$, $\tilde{x}_2(t)_{ij}$, ε_i , and ε_{ij} , each term of the sum above can be bounded. For example, if $p_{ij} > 0$, $\tilde{x}_1(t)_i \geq \varepsilon_i$, and $\tilde{x}_1(t)_j \geq \varepsilon_j$, then

$$\begin{aligned} p_{ij} (\mathbb{E}[x_i(t)x_j(t)] - \mathbb{E}[x_i(t)]\mathbb{E}[x_j(t)]) \leq \\ p_{ij} (\tilde{x}_2(t)_{ij} + \varepsilon_{ij} - (\tilde{x}_1(t)_i - \varepsilon_i)(\tilde{x}_1(t)_j - \varepsilon_j)). \end{aligned}$$

Similar bounds can easily be found in all other cases.

In particular, if we know exact values for $\mathbb{E}[x_i(t)]$ and $\mathbb{E}[x_i(t)x_j(t)]$ (i.e., if $N_T \geq 2d_S^t$), we have:

Corollary 5.2. *Let $\|\cdot\|_P$ be the P -seminorm. If $N_T \geq 2d_S^t$, for any $\alpha > \varepsilon_P$,*

$$\begin{aligned} \mathbb{P}(\|x(t) - \tilde{x}_1(t)\|_P \geq \alpha) \\ \leq \frac{\sum_{i,j=1}^n p_{ij} (\tilde{x}_2(t)_{ij} - \tilde{x}_1(t)_i \tilde{x}_1(t)_j)}{(\alpha - \varepsilon_P)^2}. \end{aligned} \quad (15)$$

One part that we have left open is how to compute a value for ε_P . In Section 4.3, we have given bounds on $\|\mathbb{E}[x(t)] - \tilde{x}_1(t)\|_\infty$. This directly gives us bounds on

$\|\mathbb{E}[x(t)] - \tilde{x}_1(t)\|_P$, using the fact that $\|x\|_P \leq \lambda_n^{1/2} \|x\|_\infty$, where λ_n is the greatest eigenvalue of P . Therefore, $\varepsilon_P \leq \lambda_n^{1/2} \varepsilon$, where ε is as defined in Section 4.3.

5.2 Computation of Probabilistic Ellipsoid Bounds

Using the bounds above, we explain how to compute probabilistic ellipsoid bounds, i.e., ellipsoid areas in which we know the system will be with at least a given fixed probability.

The problem we are interested in is the following: given a probabilistic system as in (1), approximations $\tilde{x}_1(t)$ and $\tilde{x}_2(t)$ of first and second moments of the system at time t , bounds on the errors of these approximations, and a probability p , find the largest ellipsoid in which we know the system will be with probability at least p . This can be formulated as the following optimization problem:

$$\begin{aligned} & \text{maximize } \det(P^{-1}) \text{ under} \\ & P \text{ positive-definite} \\ & \frac{\sum_{i,j=1}^n p_{ij} (\mathbb{E}[x_i(t)x_j(t)] - \mathbb{E}[x_i(t)]\mathbb{E}[x_j(t)])}{(\alpha - \varepsilon_P)^2} \leq p \end{aligned} \quad (16)$$

for some fixed $\alpha > 0$, say 1. Then, as a consequence of Proposition 5.1, the system will be in $\{x \in \mathbb{R}^{ds} \mid \|x\|_P \leq \alpha\}$ at time t with probability at least p . The actual value of α does not matter if $\varepsilon_{\lambda P} = \lambda \varepsilon_P$, which is a reasonable assumption.

Note that we are in general not interested in optimizing all dimensions of P . For example, if a system has (x, y, θ) as coordinates, we may be only interested in finding a bound for (x, y) . Maximizing $\det(P^{-1})$ under the constraints in (16) can lead to a P with a large unit ball in the θ dimension, but small in the x and y dimensions, while there may be a better P when considering just (x, y) . Let $I \subseteq \{1, \dots, n\}$ be the set of dimensions of interest, our goal is to maximize $\det(P_I^{-1})$ under the constraints above, where P_I is the submatrix of P whose indices are in I .

The problem (16) cannot be solved by convex optimization methods – and therefore not solved online – because ε_P depends on P and the presence of ε_P makes it unclear whether the constraint is convex. Moreover, computing ε_P cannot be done online repeatedly.

Hence, we propose a two-step approximate solution for efficiency. We first solve the problem above, assuming all errors are 0:

$$\begin{aligned} & \text{maximize } \det(P_I^{-1}) \text{ under} \\ & P_I \text{ positive-definite} \\ & \frac{\sum_{i,j=1}^n p_{ij} (\tilde{x}_2(t)_{ij} - \tilde{x}_1(t)_i \tilde{x}_1(t)_j)}{\alpha^2} \leq p. \end{aligned} \quad (17)$$

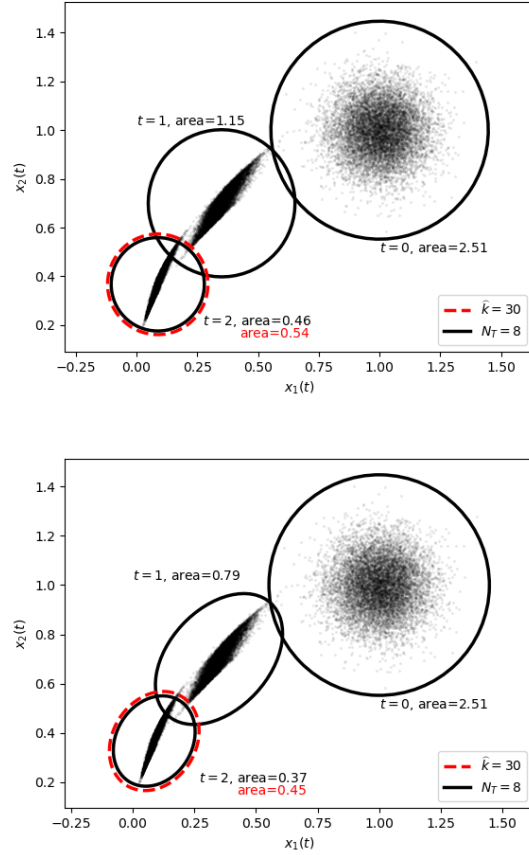


Fig. 2. Safe ball (top) and ellipsoid (bottom) bounds for safe regions with probability 0.9 for the system in Example 1, where $x(0)$ is a Gaussian random variable of mean 1 and standard deviation 0.1, and $a(t)$, $t \in \mathbb{N}$, are independent and identically distributed uniformly random variables on $[0.3, 0.4]$. The black bonds are tight bounds computed using $N_T = 8$. The red dashed bound is computed using an approximate dynamics from Proposition 4.3 with $N_T = 6$ and K consisting of $\hat{k} = 30$ indices k whose $|\tilde{y}_k|$ is the largest.

This makes the problem convex (Boyd and Vandenberghe, 2004), so it can be solved online. Our method thus consists in first solving (17), and then, in a second step, in computing ε_P for the solution to the first step and take the ellipsoid $\{x \in \mathbb{R}^{ds} \mid \|x - \tilde{x}_1(t)\|_P \leq \alpha + \varepsilon_P\}$.

Example 4. Figure 2 shows the safe regions with probability 0.9 for the system in Example 1 at time steps $t \in \{0, 1, 2\}$, plotted in comparison to 10000 Monte Carlo simulations. Both plots are computed using (17); however, in the top one, the regions are computed for $P = I_{ds}$ (i.e., ball-shaped regions). The black solid bounds are computed using $N_T = 8$; therefore, they are tight bounds where $\varepsilon = 0$ (see Proposition 4.1). The red dashed bound at time step $t = 2$ is computed using a truncated dynamics and the upper bound of its error computed as in Proposition 4.3, where the truncation limit is $N_T = 6$ and the set K consists of $\hat{k} = 30$ indices

k whose $|\tilde{y}_k|$ is the largest. Notice that the bound that we compute using the truncated dynamics and the upper bound of its error (the red one) is an over-approximation of the tight bound (the black one). Notice also that the areas of the ellipsoids are smaller than those of the ball-shaped regions (e.g., at $t = 1$, the area of the ball is 1.15, while that of the ellipsoid is 0.79).

6 Smaller matrices with reduced Kronecker powers

The main bottleneck of our method is the size of the matrix E we compute offline. One reason for this is due to duplications of computations. Indeed, the Kronecker power of a vector contains several times the same element. For example, the Kronecker square of the vector $x = \begin{bmatrix} a & b \end{bmatrix}^\top$ is given by $x^{[2]} = \begin{bmatrix} a^2 & ab & ba & b^2 \end{bmatrix}^\top$ and $ab = ba$ appears twice. In this section, we describe a *reduced Kronecker power* whose elements are the same as the normal Kronecker power, but without any duplication. For example, the reduced Kronecker square of x above will be $x^{(2)} = \begin{bmatrix} a^2 & ab & b^2 \end{bmatrix}^\top$.

Fix a vector $x = \begin{bmatrix} x_1 & \dots & x_n \end{bmatrix}^\top \in \mathbb{R}^n$. Each element of a reduced Kronecker power of x will correspond to a n -tuple of natural number (m_1, \dots, m_n) , this element being given by $x_1^{m_1} \dots x_n^{m_n}$. The degree of such an n -tuple is given by the sum of its elements $\sum_{i=1}^n m_i$. Denote the set of n -tuples of degree m by $\mathcal{I}_{n,m}$. This set can be totally ordered by lexicographic order, that is, $(m_1, \dots, m_n) < (m'_1, \dots, m'_n)$ if there is k such that $m_k < m'_k$ and for all $j < k$, $m_j = m'_j$. For example, $\mathcal{I}_{2,2} = \{(2,0) > (1,1) > (0,2)\}$.

The m -th reduced Kronecker power of x is then given by:

$$x^{(m)} = \begin{bmatrix} x_1^{m_1} \dots x_n^{m_n} \mid (m_1, \dots, m_n) \in \mathcal{I}_{n,m} \end{bmatrix}^\top. \quad (18)$$

This means that the first element of $x^{(m)}$, namely x_1^m , is given by the smallest element of $\mathcal{I}_{n,m}$, namely $(m, 0, \dots, 0)$, the second element, namely $x_1^{m-1}x_2$, is given by the second smallest element of $\mathcal{I}_{n,m}$, namely $(m-1, 1, 0, \dots, 0)$, and so on. As claimed earlier, the reduced square of $x = \begin{bmatrix} a & b \end{bmatrix}^\top$ is indeed $x^{(2)} = \begin{bmatrix} a^2 & ab & b^2 \end{bmatrix}^\top$.

Using this reduced Kronecker power, we can describe our original system in the form

$$x(t+1) = \sum_{i=0}^{d_S} \hat{F}_i(t) x^{(i)}(t), \quad t \in \mathbb{N}, \quad (19)$$

$$x(0) = x_{\text{ini}}.$$

Compared to (1), where F_i is a matrix of size $n \times n^i$, \hat{F}_i is of size $n \times |\mathcal{I}_{n,i}|$ obtained from F by summing columns.

For example, if (1) is of the form:

$$\begin{bmatrix} x_1(t+1) \\ x_2(t+1) \end{bmatrix} = \begin{bmatrix} a_{1,1} & a_{1,2} & a_{1,3} & a_{1,4} \\ a_{2,1} & a_{2,2} & a_{2,3} & a_{2,4} \end{bmatrix} \begin{bmatrix} x_1(t)^2 \\ x_1(t)x_2(t) \\ x_2(t)x_1(t) \\ x_2(t)^2 \end{bmatrix},$$

Then (19) is of the form:

$$\begin{bmatrix} x_1(t+1) \\ x_2(t+1) \end{bmatrix} = \begin{bmatrix} a_{1,1} & a_{1,2} + a_{1,3} & a_{1,4} \\ a_{2,1} & a_{2,2} + a_{2,3} & a_{2,4} \end{bmatrix} \begin{bmatrix} x_1(t)^2 \\ x_1(t)x_2(t) \\ x_2(t)^2 \end{bmatrix}.$$

Everything we described in the previous sections can be accommodated with this new power, reducing the size of the vectors and the matrices involved. More details on the saved space will be given in the experiment section.

In terms of implementation, this power relies on manipulating and generating the elements of $\mathcal{I}_{n,m}$ on the lexicographic order. This can be done by representing the n -tuples as monomials and most calculations can be done using abstract polynomials operations. In our implementation, we heavily used the python package `numpoly`¹.

7 Experimental Results

In this section, we provide two numerical examples and experimental results to illustrate our techniques.

7.1 Stochastic Logistic Map

Consider the stochastic logistic map as studied by (Athreya and Dai, 2000), which is given by

$$x(t+1) = r(t)x(t)(1-x(t)), \quad t \in \mathbb{N},$$

$$x(0) = x_0,$$

where $x_0, r(0), r(1), \dots$ are mutually independent random variables; x_0 takes values in $[0, 1]$ and $r(t)$ all take values in $[0, 4]$. The scalar $x(t) \in [0, 1]$ represents the population of a species subject to growth rate $r(t)$. This system can equivalently be represented by (1) with $d_S = 2$, $F_0(t) = 0$, $F_1(t) = r(t)$, and $F_2(t) = -r(t)$.

For experiments, we chose all $r(t)$ to be uniformly distributed over the interval $[0.4, 0.6]$, and x_0 to follow a normal distribution of mean 0.5 and standard deviation 0.1 truncated to $[0, 1]$.

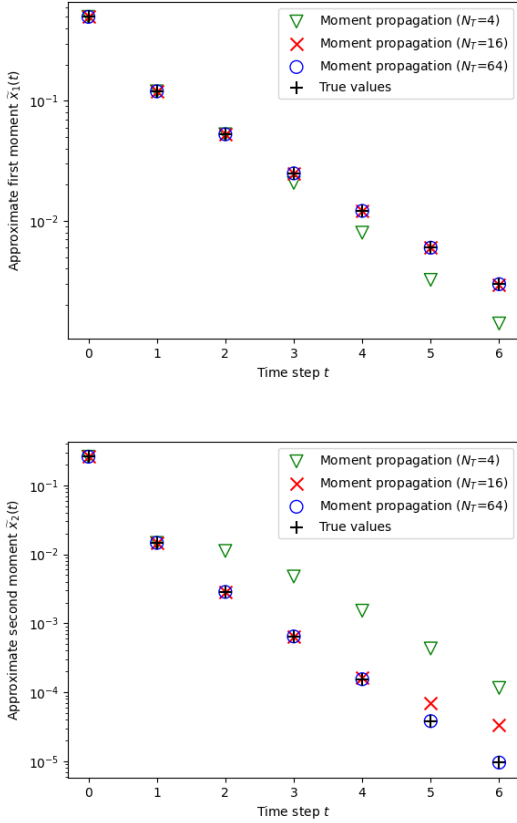


Fig. 3. Moment approximations for stochastic logistic map.

7.1.1 Moment Approximation via Truncated System

We first compare our moment approximations for different truncation limits to the true value of the moments (computed using our method with $N_T = 256$). In Figure 3, we plot the first and second moments of the truncated system with different truncation limits N_T . We observe that the system with the higher truncation limit gives a better approximation. There is one exception in the second moment approximation at $t = 6$; the system with the lower limit gives a better approximation. We also observe that larger N_T is required to obtain good approximations of higher moments. This is a natural consequence, as truncation discards more information on the dynamics of higher moments.

7.1.2 Error Bound on Moment Approximations

Next, we evaluate our approximation method of error bounds for moments. Figure 4 shows error bounds given by Proposition 4.2 with different sizes of J , with parameters $N_T = 16$, $t = 4$, and $j_0 = 2$. The index set J contains the indices j where $\|\mathbb{E}[x_0^{[j]}\|]$ is the largest, i.e., $J = \{0, \dots, |J| - 1\}$. We observe that the error bound quickly decreases as $|J|$ increases. This supports our expectation that we can use our

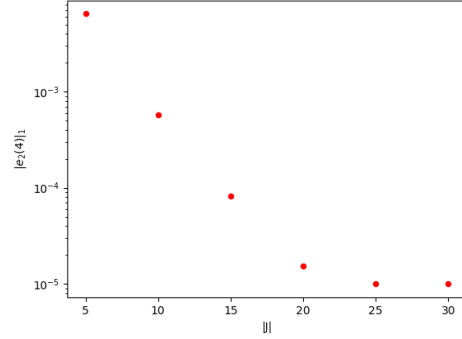


Fig. 4. Error bound on moment approximations.

error bounds for tail probability analysis with larger parameters (t , N_T , and d_S).

7.1.3 Tail Probability Analysis

Lastly, we provide a result on tail probability analysis via the method in Section 5. We computed the error bound for $0 \leq t \leq 5$ using Proposition 4.2 with $N_T = 16$ and $|J| = 6t$, where J is taken in the same way as the previous section. The results of the analysis are depicted in Figure 5. Red intervals indicate the 95%-probability neighborhoods of $\tilde{x}_1(t)$ computed by using Proposition 5.1. Blue intervals with a solid line indicate the region where 95% of 10000 Monte Carlo simulations closest to its mean belong. Dotted intervals indicate the range of 10000 Monte Carlo simulations.

We observe that the size of safety intervals given by our tail probability analysis is reasonably small. It becomes cruder in later time steps, especially at $t = 5$. This is expected, as the approximation error of moments, which is a bottleneck in refining the error bounds, becomes larger as time progresses (cf. approximate 2nd moment in Fig. 3).

There are two major advantages of our method compared to Monte Carlo simulation. One is that our technique computes moment approximations much faster than Monte Carlo (even for large N_T and a small number of samples) because we do not rely on generating random numbers. This advantage is highlighted in Table 1, which contains the online computation times for Monte Carlo simulations and our approach, averaged over 100 runs on a standard laptop computer (MacBook Pro, M1 chip, 16G memory). Another advantage is that our safety interval gives a theoretical guarantee on probabilistic safety that cannot be achieved by Monte Carlo simulations.

7.2 Application to Automated Driving

Our second example is an application to automated driving. For safety guarantees, autonomous vehicles need to predict their future positions. One way to achieve this is set-based reachability, as advocated by Althoff and Dolan (2014). To use their method, they must consider systems with bounded

¹ <https://pypi.org/project/numpoly/>

Table 1. Comparison of online computation times.

Method	Monte Carlo		Moment propagation			
Parameters	num. samples		N_T			
	10	10^4	4	16	64	256
Time (μs)	$4.4e10^3$	$2.8e10^5$	49	51	57	67

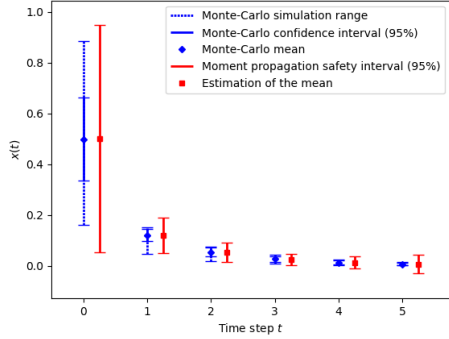


Fig. 5. Tail probability analysis with Monte-Carlo simulation and moment propagation with truncation limit $N_T = 16$.

disturbances and use linearization around an equilibrium, that is, they approximate a polynomial system by a linear one, using Lagrange remainders. Our method is based on Carleman linearization, which allows taking the effect of higher dimensions of the system into account more precisely than Lagrange remainders. Moreover, our approach is probabilistic, while theirs is set-based, so the two approaches give different types of guarantees.

We consider a scenario in which, at each time step, the autonomous vehicle measures its current position with some known sensor error distributions, computes moments of its current state based on this measurement and the known error distribution, and predicts its future positions (and moments) up to t steps ahead in time by applying the truncated system to these moments.

7.2.1 Vehicle Dynamics

More precisely, we consider the *kinematic bicycle model* of a vehicle from Kong *et al.* (2015), which we rewrite as the following equivalent polynomial system

$$\begin{aligned} \dot{p}_x(t) &= v(t)c(t), & \dot{p}_y(t) &= v(t)s(t), \\ \dot{\psi}(t) &= \frac{v(t)}{\ell} \sin \beta, & \dot{v}(t) &= a(t), \\ \dot{c}(t) &= -\frac{s(t)v(t) \sin \beta}{\ell}, & \dot{s}(t) &= \frac{c(t)v(t) \sin \beta}{\ell}, \end{aligned}$$

for $t \geq 0$, where $p_x(t) \in \mathbb{R}$ and $p_y(t) \in \mathbb{R}$ represent the X-Y coordinates of the mass-center of the vehicle, $v(t) \in \mathbb{R}$ denotes its speed, $\psi(t)$ its inertial heading, and $a(t) \in \mathbb{R}$

its acceleration. The constants $\beta \in \mathbb{R}$ and $\ell > 0$ respectively denote the angle of velocity and the distance from the vehicle's rear axle to its mass-center. The scalars $c(t)$ and $s(t)$ are auxiliary variables that are introduced to obtain the polynomial model above from the original model of Kong *et al.* (2015) (which involves trigonometric terms), using the same techniques as Carothers *et al.* (2005).

The second-order Taylor expansion of the model above gives the following discrete-time approximation:

$$\begin{aligned} p_x(t + \Delta) &= p_x(t) + \Delta c(t)v(t) \\ &\quad + \frac{\Delta^2}{2} \left(a(t)c(t) - \frac{s(t)v^2(t) \sin \beta}{\ell} \right), \\ p_y(t + \Delta) &= p_y(t) + \Delta s(t)v(t) \\ &\quad + \frac{\Delta^2}{2} \left(a(t)s(t) + \frac{c(t)v^2(t) \sin \beta}{\ell} \right), \\ \psi(t + \Delta) &= \psi(t) + \Delta \frac{v(t)}{\ell} \sin \beta + \frac{\Delta^2}{2} \frac{a(t)}{\ell} \sin \beta, \\ v(t + \Delta) &= v(t) + \Delta a(t), \\ c(t + \Delta) &= c(t) - \Delta \frac{s(t)v(t) \sin \beta}{\ell} \\ &\quad - \frac{\Delta^2}{2} \left(\frac{c(t)v^2(t) \sin^2 \beta}{\ell^2} + \frac{a(t)s(t) \sin \beta}{\ell} \right), \\ s(t + \Delta) &= s(t) + \Delta \frac{c(t)v(t) \sin \beta}{\ell} \\ &\quad + \frac{\Delta^2}{2} \left(-\frac{s(t)v^2(t) \sin^2 \beta}{\ell^2} + \frac{a(t)c(t) \sin \beta}{\ell} \right), \end{aligned}$$

where $\Delta > 0$. To describe the evolution of the states of the vehicle at times $0, \Delta, 2\Delta, \dots$, we write this system in the form of (1). In particular, consider the discrete-time instant $t \in \mathbb{N}$ corresponding to the continuous time $t\Delta$. By letting

$$x(t) \triangleq [p_x(t), p_y(t), \psi(t), v(t), c(t), s(t)]^\top,$$

we obtain (1) where $d_S = 3$ and the coefficients $F_0(t), \dots, F_3(t)$ depend on Δ, β, ℓ , and $a(t)$. We consider the setting where the acceleration values $a(0), a(1), \dots$ are independent uniformly-distributed random variables over $[0.9, 1]$, $\Delta = 0.1$, $\beta = \pi/8$, $\ell = 2.5$, and, for the initial state, $p_x(0), p_y(0), v(0), \psi(0)$ are independent Gaussian random variables with mean 0 and standard deviation 0.1, and $c(0) = \cos(\psi(0) + \beta)$ and $s(0) = \sin(\psi(0) + \beta)$.

7.2.2 Experimental Results

Figure 6 shows the expected trajectory of the vehicle as approximated by our method for different truncation limits, as well as the empirical distribution computed by 10000 runs of Monte Carlo simulation and the mean of that distribution. Figure 7 shows the distance between $\tilde{x}_1(t)$ and the mean of the empirical distribution for the same truncation limits.

Figures 6 and 7 show that larger truncation limits give truncated systems that follow the empirical distribution closer.

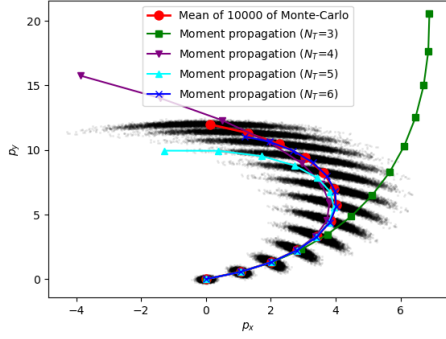


Fig. 6. First moment approximation of vehicle dynamics.

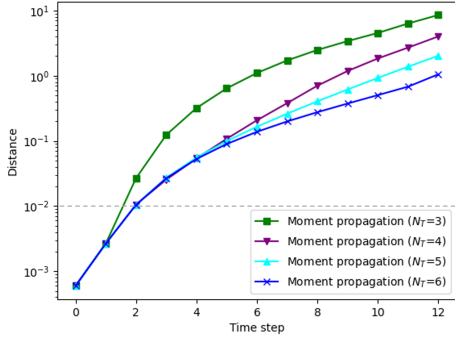


Fig. 7. Distance to the mean of the empirical distribution.

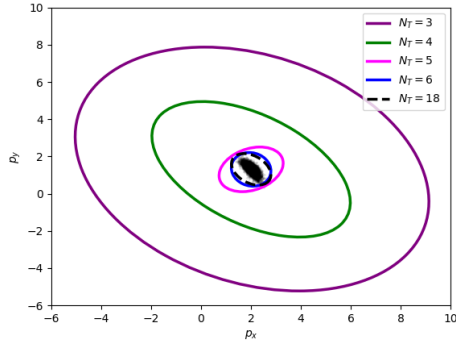


Fig. 8. The ellipsoids of the safe region for time step 2 and probability bound 0.9 computed using (16) and Proposition 4.3 with $\hat{k} = 4500$ and different truncation limits N_T . Using $N_T = 18$, we obtain the region computed using the exact moments (see Proposition 4.1).

It also shows that, for a fixed truncation limit, the distance to the empirical system grows larger with time. Note that, by Proposition 4.1, using $N_T = 6$ gives an exact computation at $t = 2$, which means that the error at this point (corresponding to the horizontal line in Figure 7) is entirely induced by Monte Carlo. Therefore, it is pointless to consider errors that are of the same order as the one introduced by Monte Carlo at $t = 2$.

Figure 8 shows the ellipsoids of the safe region at time

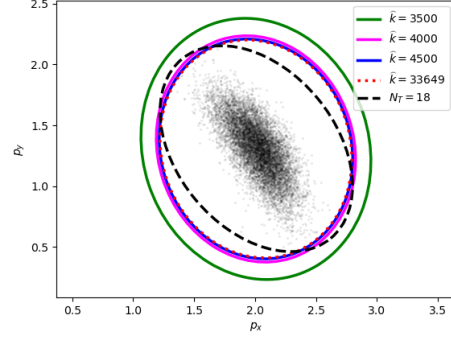


Fig. 9. The ellipsoids of the safe region for time step 2 and probability bound 0.9 computed using (16) and Proposition 4.3 with $N_T = 6$ and different sets K . Each ellipsoid is computed using the set K consists of \hat{k} indices k where $|\hat{y}_k|$ is the largest. Using $N_T = 18$, we obtain the region computed using the exact moments (see Proposition 4.1).

step 2 with probability bound 0.9 computed using (16) and Proposition 4.3 with different truncation limits N_T . We use the set K (in Proposition 4.3) that contains $\hat{k} = 4500$ indices k where $|\hat{y}_k|$ is the largest. Figure 9 also shows the ellipsoids of the safe region at time step 2 with probability bound 0.9, but with different index sets K . We can see that the larger K is, the ellipsoids get closer to that obtained with the exact computation using $N_T = 8$ and Proposition 4.1 (the black dashed bound). Note that the set K containing all 33,649 indices means that it contains all moments needed for an exact computation of the upper bound of truncation error at $t = 2$ (for $N_T = 6$) using (9) and the reduced Kronecker powers in Section 6. In other words, the red dotted bound is the tightest bound we can obtain using our method for the truncation limit $N_T = 6$. We note that the bound computed with $\hat{k} = 4000$ and $\hat{k} = 4500$ are very close to this tightest bound and their computation is much faster.

7.3 Comparison of Kronecker Powers and Reduced Kronecker Powers

In Section 7.2, we used the reduced Kronecker powers described in Section 6 to generate the matrices $E(N_T, N_T)$. Here, we illustrate the gain – both in time and space – obtained by using reduced Kronecker powers instead of non-reduced ones. The comparison results are compiled in Figure 10 (run on a MacBook Pro, M1 chip, 16G memory).

We compared the following performance indicators (from top to bottom plots), for $N_T \in \{2, \dots, 7\}$:

- The time to compute $E(N_T, N_T)$.
- The size of the compressed data file (pickled npz format in Numpy/Python) containing $E(N_T, N_T)$.
- The number of rows of $E(N_T, N_T)$.
- The time required to compute $\hat{y}(10)$.

We remark that using reduced Kronecker powers significantly improves the performance in all aspects, making both

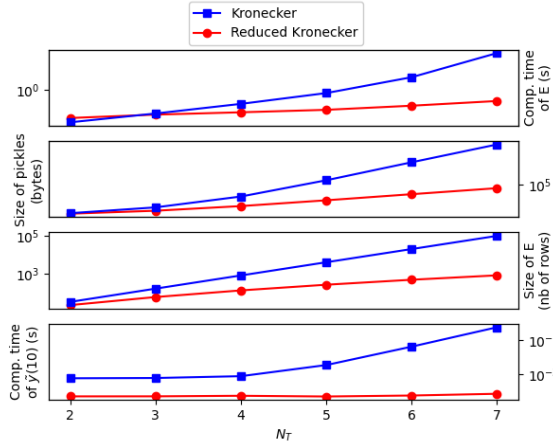


Fig. 10. Comparison between Kronecker powers and reduced ones

the online and the offline computations much faster, and the memory load much lighter. Furthermore, we also note that the computation of $E(8,8)$ using non-reduced Kronecker powers reached an out-of-memory error after several hours of computation, while we could compute $E(25,25)$ in less than an hour with reduced ones.

8 Conclusions

In this paper, we have proposed a method to approximate the moments of a discrete-time stochastic polynomial system. This method is built upon a Carleman linearization approach with truncation, where approximate moments are obtained by propagating initial moments through a finite-dimensional linear deterministic difference equation. We have presented guaranteed bounds on the approximation errors. We have then used the approximate moments and the approximation error bounds together with a convex optimization technique to provide probabilistic safety analysis.

Our moment approximation method is applicable to systems with both additive and multiplicative noise. Furthermore, it provides probabilistic guarantees even when the dynamics and the noise probability distributions are complicated. We have demonstrated our method on a stochastic logistic map and a vehicle model with stochastic acceleration inputs.

Our method involves computations in two phases: an initial offline computation phase where the approximate moment dynamics are obtained, and an online computation phase that involves propagation of the initial moments through the obtained dynamics. The online phase is very fast and we have shown in our numerical examples that our method can provide moment approximations in much shorter times compared to the Monte Carlo approach based on repeated simulations. For the offline computations, we have investigated a technique to improve the efficiency by using the symmetry of Kronecker powers and reducing the sizes of the matrices involved in the computations.

While in this paper we have addressed only polynomial sys-

tems, our method can also be applied to certain nonpolynomial systems. In some cases, nonpolynomial dynamics can be transformed to polynomial ones by introducing auxiliary variables, as illustrated in one of our numerical examples. In other cases, polynomial approximations can be useful.

We have used the approximated moments of the system's state for computing tail-probability bounds of the state being outside of ellipsoidal safety regions. As pointed out by Schmüdgen (2017) and John *et al.* (2007), approximate moments of random variables can be useful for approximating probability distributions. One of our future research directions is to investigate approximation of the probability distribution of the system state by using its approximated moments.

References

- Al-Tuwaim, Mohammad S, Oscar D. Crisalle and Spyros A. Svoronos (1998). Discretization of nonlinear models using a modified Carleman linearization technique. In: *Proceedings of the 1998 American Control Conference. ACC (IEEE Cat. No. 98CH36207)*. Vol. 5. IEEE. pp. 3084–3088.
- Althoff, Matthias and John M. Dolan (2014). Online Verification of Automated Road Vehicles Using Reachability Analysis. *IEEE Trans. Robotics* **30**(4), 903–918.
- Amini, Arash, Qiyu Sun and Nader Motee (2019). Carleman State Feedback Control Design of a Class of Nonlinear Control Systems. *IFAC-PapersOnLine* **52**(20), 229–234. 8th IFAC Workshop on Distributed Estimation and Control in Networked Systems NECSYS 2019.
- Amini, Arash, Qiyu Sun and Nader Motee (2020). Quadraticization of Hamilton-Jacobi-Bellman Equation for Near-Optimal Control of Nonlinear Systems. In: *59th IEEE Conference on Decision and Control, CDC 2020, Jeju Island, South Korea, December 14–18, 2020*. IEEE. pp. 731–736.
- Athreya, Krishna B. and Jack Dai (2000). Random Logistic Maps. I. *Journal of Theoretical Probability* **13**(2), 595–608.
- Banzhaf, Holger, Maxim Dolgov, Jan Erik Stellet and J. Marius Zöllner (2018). From Footprints to Beliefprints: Motion Planning under Uncertainty for Maneuvering Automated Vehicles in Dense Scenarios. In: *21st International Conference on Intelligent Transportation Systems, ITSC 2018, Maui, HI, USA, November 4–7, 2018* (Wei-Bin Zhang, Alexandre M. Bayen, Javier J. Sánchez Medina and Matthew J. Barth, Eds.). IEEE. pp. 1680–1687.
- Bellman, Richard (1970). *Introduction to matrix analysis*. Chap. 12, pp. 236–237. 2nd ed.. McGraw-Hill. New York.
- Bellman, Richard and John M. Richardson (1963). On some questions arising in the approximate solution of nonlinear differential equations. *Quarterly of Applied Mathematics* **20**(4), 333–339.
- Boyd, Stephen and Lieven Vandenberghe (2004). *Convex optimization*. Cambridge University Press.
- Bry, Adam and Nicholas Roy (2011). Rapidly-exploring Random Belief Trees for Motion Planning Under Uncertainty. In: *IEEE International Conference on Robotics and Automation, ICRA 2011, Shanghai, China, May 9–13, 2011*. IEEE. pp. 723–730.
- Cacace, Filippo, Valerio Cusimano, Alfredo Germani and Pasquale Palumbo (2014). A Carleman discretization approach to filter nonlinear stochastic systems with sampled measurements. *IFAC Proceedings Volumes* **47**(3), 9534–9539. 19th IFAC World Congress.

- Cacace, Filippo, Valerio Cusimano, Alfredo Germani, Pasquale Palumbo and Marco Papi (2017). Optimal linear filter for a class of nonlinear stochastic differential systems with discrete measurements. In: *56th IEEE Annual Conference on Decision and Control, CDC 2017, Melbourne, Australia, December 12–15, 2017*. IEEE. pp. 2807–2812.
- Carothers, David C, G Edgar Parker, James S Sochacki and Paul G Warne (2005). Some properties of solutions to polynomial systems of differential equations. *Electronic Journal of Differential Equations* **2005**(40), 1–17.
- Carravetta, Francesco, Alfredo Germani and Massimo Raimondi (1996). Polynomial filtering for linear discrete time non-Gaussian systems. *SIAM Journal on Control and Optimization* **34**(5), 1666–1690.
- Cibulka, Vít, Tomáš Haniš, Milan Korda and Martin Hromčík (2020). Model Predictive Control of a Vehicle using Koopman Operator. *IFAC-PapersOnLine* **53**(2), 4228–4233.
- Forets, Marcelo and Amaury Pouly (2017). Explicit Error Bounds for Carleman Linearization. *CoRR*.
- Goswami, Debdipta and Derek A. Paley (2017). Global bilinearization and controllability of control-affine nonlinear systems: A Koopman spectral approach. In: *56th IEEE Annual Conference on Decision and Control, CDC 2017, Melbourne, Australia, December 12–15, 2017*. IEEE. pp. 6107–6112.
- Gray, Henry L. and Suojin Wang (1991). A General Method for Approximating Tail Probabilities. *Journal of the American Statistical Association* **86**(413), 159–166.
- Hashemian, Negar and Antonios Armaou (2019). Feedback control design using model predictive control formulation and Carleman approximation method. *AIChE Journal* **65**(9), 1–11.
- Jasour, Ashkan, Allen Wang and Brian C. Williams (2021). Moment-Based Exact Uncertainty Propagation Through Nonlinear Stochastic Autonomous Systems. *CoRR*.
- John, V., I. Angelov, A.A. Öncül and D. Thévenin (2007). Techniques for the reconstruction of a distribution from a finite number of its moments. *Chem. Eng. Sci.* **62**(11), 2890–2904.
- Kong, Jason, Mark Pfeiffer, Georg Schildbach and Francesco Borrelli (2015). Kinematic and dynamic vehicle models for autonomous driving control design. In: *2015 IEEE Intelligent Vehicles Symposium, IV 2015, Seoul, South Korea, June 28 – July 1, 2015*. IEEE. pp. 1094–1099.
- Laub, Alan J. (2004). *Matrix Analysis For Scientists And Engineers*. Society for Industrial and Applied Mathematics.
- Mesbahi, Afshin, Jingjing Bu and Mehran Mesbahi (2019). On Modal Properties of the Koopman Operator for Nonlinear Systems with Symmetry. In: *2019 American Control Conference, ACC 2019, Philadelphia, PA, USA, July 10–12, 2019*. IEEE. pp. 1918–1923.
- Pruekprasert, Sasinee, Toru Takisaka, Clovis Eberhart, Ahmet Cetinkaya and Jérémy Dubut (2020). Moment Propagation of Discrete-Time Stochastic Polynomial Systems using Truncated Carleman Linearization. *IFAC-PapersOnLine* **53**(2), 14462–14469. 21st IFAC World Congress.
- Rauh, Andreas, Johanna Minisini and Harald Aschemann (2009). Carleman Linearization for Control and for State and Disturbance Estimation of Nonlinear Dynamical Processes. *IFAC Proceedings Volumes* **42**(13), 455–460. 14th IFAC Conference on Methods and Models in Automation and Robotics.
- Schmüdgen, K. (2017). *The Moment Problem*. Springer.
- Shen, Xun, Xingguo Zhang and Pongsathorn Raksincharoensak (2020). Probabilistic Bounds on Vehicle Trajectory Prediction Using Scenario Approach. *IFAC-PapersOnLine* **53**(2), 2385–2390. 21st IFAC World Congress.
- Steeb, W.-H. and F. Wilhelm (1980). Non-linear autonomous systems of differential equations and carleman linearization procedure. *Journal of Mathematical Analysis and Applications* **77**(2), 601–611.
- Wong, Wing Shing (1983). Carleman linearization and moment equations of nonlinear stochastic equations. *Stochastics* **9**(1-2), 77–101.